






# Mathematical analysis and forecasting of controlled Spatio-temporal dynamics of the EG.5 Virus

E. M. Moumine\*, , O. Balatif  and M. Rachik 

## Abstract

In this article, we propose a mathematical approach that connects an innovative spatio-temporal model to the problem of the **EG.5** variant of COVID-19 in a human population. We demonstrate the existence and

---

\*Corresponding author

Received ??? ; revised ??? ; accepted ???

El Mehdi Moumine

Laboratory of Analysis, Modeling and Simulation, Department of Mathematics and Computer Science, Faculty of science Ben M'sik, University Hassan II, Casablanca, Morocco. e-mail: moumine.maths@gmail.com

Omar Balatif

Laboratory of Fundamental Mathematics and Their Applications , Department of Mathematics Faculty of Sciences El Jadida, Chouaib Doukkali University, El Jadida, Morocco. e-mail: balatif.maths@gmail.com

Mostafa Rachik

Laboratory of Analysis, Modeling and Simulation, Department of Mathematics and Computer Science, Faculty of science Ben M'sik, University Hassan II, Casablanca, Morocco. e-mail: m\_rachik@yahoo.fr

## How to cite this article

Moumine, E.M., Balatif, O. and Rachik, M., Mathematical analysis and forecasting of controlled Spatio-temporal dynamics of the EG.5 Virus. *Iran. J. Numer. Anal. Optim.*, ??; ??(??): ??-??. ??

uniqueness of the global positive solution for our suggested system. The implementation and analysis of an applicable optimal control issue are as follows. The methods of optimal control theory are applied in this work to demonstrate the existence of optimal control, and with necessary optimality conditions, we discover the explicit expression of optimal control that minimizes the negative impacts of this infectious disease on countries. We provide numerical simulations at the conclusion to demonstrate the efficacy of our chosen strategy.

**AMS subject classifications (2020):** 49J15, 92B05, 93A30, 93C10

**Keywords:** Spatio-temporal Model; EG.5 Virus; Optimal Control; Mathematical Model.

## 1 Introduction

The COVID-19 pandemic swept into our world suddenly, causing global disruption and emphasizing the need for cutting-edge scientific methods to understand and stop the spread of the disease. Among these methods, quantitative analysis and optimal control are essential for understanding the spatio-temporal spread of the virus and formulating powerful strategies to fight the epidemic.

Since the discovery of the first cases in December 2019, the epidemic has wreaked havoc on the economy, society, and public health worldwide. The disease quickly crossed international borders, confounding health agencies and efficiencies around the world. Scientists and researchers have used mathematical techniques to study the dynamics of the spread of COVID-19 and formulate customized public health policies in this fight against an implacable foe (see [15, 9, 2, 12, 1, 14, 16, 23, 11, 10, 7, 8, 21, 18, 3]). Although the pandemic might appear to be a distant recollection for some, the coronavirus persists in its spread, with a surge in new cases attributed to emerging mutant strains. One such mutation, known as **EG.5**, has gained prominence in Europe since its initial detection earlier this year (2023). Recently, the world health organization (WHO) has classified it as a “variant of interest” in response to the escalating global case numbers.

EG.5 virus represents a subcategory of the Omicron variant of COVID-19 and exhibits a close genetic relationship with other globally circulating variants. It signifies a modified form of the virus. Its prevalence has surged on a global scale, rising from 7.6% of COVID-19 cases in late June to 17.4% by the close of July (2023), prompting the WHO to designate it as a matter of particular concern. Health authorities worldwide are currently conducting investigations into this novel virus. Similar to its predecessors, this fresh variant has undergone multiple mutations. Scientists are tirelessly working to grasp its attributes, encompassing its transmissibility, severity, and potential implications for vaccine efficacy. Presently, the public is strongly encouraged to persist in adhering to safety protocols, including mask-wearing, practicing social distancing, and receiving vaccinations, in order to mitigate the virus's propagation.

In addition, it is necessary to model and predict the spread of the virus and develop effective control strategies by offering theoretical models that take into account the complex interactions between people, the environment, and the properties of the virus itself. This mathematical study makes it possible to understand the spatio-temporal transmission of viruses. These mathematical models, like epidemiological models, provide a framework to analyze and predict disease progression in a specific population. Additionally, they enable quantification of the impact of various control methods such as social isolation, mask use, and vaccination on virus spread.

However, to maximize the effectiveness of control strategies, an optimal control-based strategy must be used. The goal of the latter is to select the best preventive measures considering limitations and available resources to reduce the spread of disease. This method combines mathematical analysis with optimization techniques to pinpoint actions that will have the greatest impact on reducing case incidence, mortality and the strain on the healthcare system.

In this article, the optimal management of the spatio-temporal transmission of EG.5 virus is reviewed together with current developments in the field of mathematical analysis. We look at the spread of the disease as described by the epidemiological model. We also move from optimal control strategies that we can implement in our spatio-temporal model to create effective pub-

lic health regulations that take into account the specific characteristics of the disease, available resources, and ethical considerations. In order to evaluate the outcomes of treatments and to support intelligent decision making.

## 2 Background

However, merely simply simulating how the virus spreads will not be enough to stop a pandemic. This is where it is important to have good control. The goal of optimal control is to consider the limitations and resources at hand and identify proper management methods to reduce virus spread [4, 13, 6, 17, 20]. Determining the timing and level of containment measures, vaccination campaigns, managing medical resources, or even adapting screening and research strategies are some possible solutions.

The researchers conducted an evaluation of various interventions, employing a combination of mathematical analysis and optimal control techniques to identify the most effective approaches for reducing viral transmission. In one study [15], the authors introduced a model featuring two distinct controls. The first control demonstrated an increase in the proportion of individuals adopting virus-preventive measures, coupled with a decrease in those not doing so. These changes were attributed to media campaigns and direct community engagement efforts. The second control illustrated that limiting social interactions effectively lowered disease transmission risk, subsequently reducing the number of infected individuals. In another study [9], the authors aimed to develop a multi-regional model by incorporating four alternative strategies as controls. The first control represented awareness campaigns in the region “ $j$ ,” with a focus on disseminating health precautions to protect individuals from viral infections. The second control addressed health and security measures to restrict movement between regions “ $j$ ” and “ $r$ .” The third control involved promoting quarantine measures for exposed individuals within the same regions, while the fourth aimed to eliminate infected animals.

We will examine a spatio-temporal mathematical model, which is based on the one we used in [15]. To gain deeper insights into the virus’s temporal and spatial propagation dynamics, our analysis will incorporate a spatial variable.

This integration involves introducing a diffusion term utilizing the Laplace operator (well explained in [24]). Furthermore, we will conduct an optimal control investigation to enhance our understanding. The management of the spatio-temporal transmission of EG.5 virus will then be examined, with a focus on the role of mathematical analysis and optimal control in evaluating the efficacy of current interventions, exploring novel avenues, and offering recommendations based on reliable quantitative data. By understanding the potential impact of this study, we will be better prepared to meet the future challenges linked to this world pandemic.

### 3 Model formulation

The progression of the EG.5 virus in a human population can be explained by the SEIHR model that we suggest, which is shown in Figure 1. It is clear

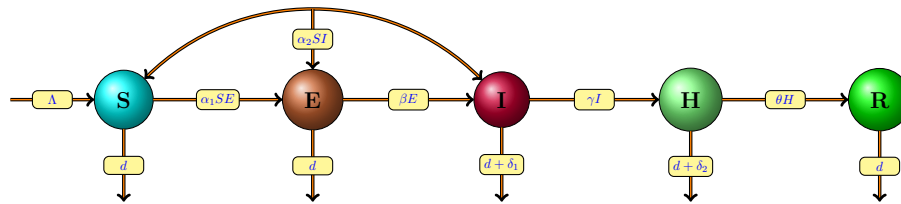


Figure 1: Diagram depicting the evolution of the EG.5 virus.

that the EG.5 virus is described in the following temporal dynamic system:

$$\begin{cases} \frac{dS(t)}{dt} = \Lambda - [\alpha_1 E(t) + \alpha_2 I(t)] S(t) - dS(t), \\ \frac{dE(t)}{dt} = [\alpha_1 E(t) + \alpha_2 I(t)] S(t) - (d + \beta) E(t), \\ \frac{dI(t)}{dt} = \beta E(t) - (d + \delta_1 + \eta) I(t), \\ \frac{dH(t)}{dt} = \eta I(t) - (d + \delta_2 + \theta) H(t), \\ \frac{dR(t)}{dt} = \theta H(t) - dR(t). \end{cases} \quad (1)$$

The different compartments of our spatio-temporal model are listed below, Table 1, indicating their descriptions (see [15]). It is clear that the temporal

Table 1: The description of the different compartments of our model.

Compartment	Description
<b>S</b>	The number of people likely to be infected by the virus.
<b>E</b>	The number of infected people who are symptomless.
<b>I</b>	The number of infected people showing symptoms
<b>H</b>	The number of hospitalized people
<b>R</b>	The number of the recovered people

dynamic system (1) cannot adequately describe how the virus spreads over the area. We advocate using the Laplacian operator to close this gap. To be specific, we add the followings to the deterministic epidemic EG.5 mode:

$$\begin{cases} \frac{dS(t, z)}{dt} = d_S \Delta S(t, z) + \Lambda - (1 - u) [\alpha_1 E(t, z) + \alpha_2 I(t, z)] S(t, z) - dS(t, z), \\ \frac{dE(t, z)}{dt} = d_E \Delta E(t, z) + (1 - u) [\alpha_1 E(t, z) + \alpha_2 I(t, z)] S(t, z) - (d + \beta) E(t, z), \\ \frac{dI(t, z)}{dt} = d_I \Delta I(t, z) + \beta E(t, z) - (d + \delta_1 + \eta) I(t, z), \\ \frac{dH(t, z)}{dt} = d_H \Delta H(t, z) + \eta I(t, z) - (d + \delta_2 + \theta) H(t, z), \\ \frac{dR(t, z)}{dt} = d_R \Delta R(t, z) + \theta H(t, z) - dR(t, z). \end{cases} \quad (2)$$

The initial conditions and no-flux boundary conditions are expressed as follows:

$$S(0, z) = S_0, E(0, z) = E_0, I(0, z) = I_0, H(0, z) = H_0, R(0, z) = R_0, \quad z \in \Omega. \quad (3)$$

Here,  $\Omega$  represents a bounded domain within  $\mathbb{R}^2$  with smooth boundary denoted as  $\partial\Omega$ . One needs to add the equation

$$\frac{\partial S}{\partial v} = \frac{\partial E}{\partial v} = \frac{\partial I}{\partial v} = \frac{\partial H}{\partial v} = \frac{\partial R}{\partial v} = 0, \quad (t, z) \in [0; t_f] \times \partial\Omega, \quad (4)$$

where  $v$  represents the outward unit normal vector on the boundary  $\partial\Omega$ , and  $\frac{\partial}{\partial v}$  corresponds to the outward normal derivative on  $\partial\Omega$ .

Additionally, we have a control function  $u : [0; t_f] \times \Omega \rightarrow [0; 1[$ , which is designed to decrease the count of infected individuals while concurrently increasing the count of susceptible individuals. This is achieved through the implementation of measures aimed at reducing social interactions, conducting

security campaigns to inhibit migration, and promoting health precautions to minimize virus transmission.

Our objective is to optimize both the count of individuals affected by the illness and the cost of the treatment program. To achieve this, we formulate the problem as follows: Minimize the cost functional represented by

$$C(S, E, I, H, R, u) = \int_{\Omega} \int_0^{t_f} aI(t, z) dt dz + \frac{b}{2} \|u(t, z)\|_{L^2([0, t_f])}^2 \quad (5)$$

subject to the controlled system (2).

Additionally, we define  $U_{ad}$  as the set of admissible controls, characterized by

$$U_{ad} = \{u \in L^\infty(Q), 0 \leq u \leq 1 \quad \text{a.e. on } Q\}, \quad (6)$$

where  $Q = [0, t_f] \times \Omega$ , with  $\Omega$  representing a bounded region within  $\mathbb{R}^2$  featuring a smooth boundary  $\partial\Omega$ . Further details about the parameters of our spatio-temporal model can be found in Table 2.

Table 2: The description of the parameters of our spatio-temporal model (2).

Symbol	Description
$\Lambda$	Recruitment rate
$d$	Natural mortality rate
$\alpha_1$	Virus transmission rate between an infected person without symptoms and a person users
$\alpha_2$	Virus transmission rate between an infected person with symptoms and a person users
$\beta$	Rate of infected person without symptoms
$\delta_1$	Infected viral mortality rate
$\delta_2$	Viral mortality rate of an infected person during hospitalization
$\eta$	Hospitalized people rate
$\theta$	Recovered rate
$d_S$	Diffusion of susceptible individuals
$d_E$	Diffusion of infected people without symptoms
$d_I$	Diffusion of infected people with symptoms
$d_H$	Diffusion of hospitalized people
$d_R$	Diffusion of recovered people

## 4 Existence and uniqueness of global solution

In this part, we demonstrate that our model (2) has a strong global solution.

We consider  $M(\Omega) = (L_2(\Omega))^5$ ,  
 $H^1(\Omega) = \left\{ u \in L_2(\Omega) : \frac{\partial u}{\partial x} \in L_2(\Omega) \text{ and } \frac{\partial u}{\partial y} \in L_2(\Omega) \right\}$ ,  
and  $H^2(\Omega) = \left\{ u \in H^1(\Omega) : \frac{\partial^2 u}{\partial y^2}, \frac{\partial^2 u}{\partial x \partial y}, \frac{\partial^2 u}{\partial y \partial x} \in L_2(\Omega) \right\}$  the Hilbert spaces.

Let  $L^2(0, t_f; H^2(\Omega))$  be the space of all strongly measurable functions  $v : [0, t_f] \mapsto H^2(\Omega)$  such that

$$\int_0^{t_f} \|v(t, z)\|_{H^2(\Omega)} dt < \infty.$$

Additionally, we define  $L^\infty(0, t_f; H^1(\Omega))$  as the set of all functions  $v : [0, t_f] \mapsto H^1(\Omega)$  that satisfy

$$\sup_{t \in [0, t_f]} (\|v(t, z)\|_{H^1(\Omega)}) < \infty.$$

The norm in  $L^\infty(0, t_f; H^1(\Omega))$  is given by

$$\|v\|_{L^\infty(0, t_f; H^1(\Omega))} := \inf \{ m \in \mathbb{R}_+ : \|v(t, z)\|_{H^1(\Omega)} < m \}.$$

Our spatio-temporal model (2) can be expressed in the following form

$$\frac{\partial y(t, z)}{\partial t} = Ay(t, z) + f(t, y(t, z)), \quad (7)$$

where  $y = (y_1, y_2, y_3, y_4, y_5) = (S, E, I, H, R)$  and  $f = (f_1, f_2, f_3, f_4, f_5)$  is defined by

$$\begin{cases} f_1 = \Lambda - (1 - u) [\alpha_1 y_2 + \alpha_2 y_3] y_1 - dy_1, \\ f_2 = (1 - u) [\alpha_1 y_2 + \alpha_2 y_3] y_1 - (d + \beta) y_2, \\ f_3 = \beta y_2 - (d + \delta_1 + \eta) y_3, \\ f_4 = \eta y_3 - (d + \delta_2 + \theta) y_4, \\ f_5 = \theta y_4 - dy_5. \end{cases}$$

For all  $k \in \{1, 2, 3, 4, 5\}$

$$\frac{\partial y_k}{\partial t} = d_k \Delta y_k + f_k(y(t, z)).$$

Let  $A$  denote the linear operator, mapping from  $D(A) \subset M(\Omega)$ , defined as follows:

$$Ay = (d_S \Delta y_1, d_E \Delta y_2, d_I \Delta y_3, d_H \Delta y_4, d_R \Delta y_5)$$



with

$$y \in D(A) = \left\{ y = (y_1, y_2, y_3, y_4, y_5) \in (H^2(\Omega))^5 : \right. \\ \left. \frac{\partial y_1}{\partial \nu} = \frac{\partial y_2}{\partial \nu} = \frac{\partial y_3}{\partial \nu} = \frac{\partial y_4}{\partial \nu} = \frac{\partial y_5}{\partial \nu} = 0 \quad \text{on} \quad \partial\Omega \right\}.$$

**Theorem 1.** Consider a bounded region  $\Omega$  in  $\mathbb{R}^2$  with a sufficiently smooth boundary. Assuming nonnegativity constraints for  $y_k^0$  on  $\Omega$  (for  $k \in \{1, 2, 3, 4, 5\}$ ), as well as nonnegative parameters  $\Lambda, d, \alpha_1, \alpha_2, \beta, \delta_1, \delta_2, \eta$ , and  $\theta$ , and an admissible control  $u \in U_{ad}$  with an initial condition  $y^0 \in D(A)$ , the system (2) possesses a unique strong nonnegative solution  $y \in W^{1,2}([0, t_f]; M(\Omega))$ , satisfying the following properties:

$$y_1, y_2, y_3, y_4, y_5 \in L^2(0, t_f; H^2(\Omega)) \cap L^\infty(0, t_f; H^1(\Omega)) \cap L^\infty(Q).$$

Moreover, there exists a constant  $M_0 > 0$ , independent of the control  $u$ , such that for all  $t \in [0, t_f]$  and all  $k \in \{1, 2, 3, 4, 5\}$

$$\left\| \frac{\partial y_k}{\partial t} \right\|_{L^2(Q)} + \|y_k\|_{L^2(0, t_f, H^2(\Omega))} + \|y_k\|_{H^1(\Omega)} + \|y_k\|_{L^\infty(Q)} \leq M_0. \quad (8)$$

*Proof.* Since the operator  $\Delta$  possesses characteristics of dissipation, self-adjointness, and the capacity to generate a  $C_0$  semigroup of contractions on  $M(\Omega)$  [22], it is readily apparent that the function  $f$  represented as  $(f_1, f_2, f_3, f_4, f_5)$  maintains Lipschitz continuity concerning the variable  $y$  denoted by  $(y_1, y_2, y_3, y_4, y_5)$ , and this continuity remains uniform with respect to  $t$  within the interval  $[0, t_f]$ . Consequently, the system possesses a unique strong solution  $y \in W^{1,2}([0, t_f]; M(\Omega))$  with

$$y_k \in L^2(0, t_f; H^2(\Omega)) \quad \text{for all } k \in \{1, 2, 3, 4, 5\}. \quad (9)$$

We prove now that for all  $k \in \{1, 2, 3, 4, 5\}$ ,  $y_k \in L^\infty(Q)$ .

Set  $c = \max \left\{ \|f_k\|_{L^\infty(Q)}, \|y_k^0\|_{L^\infty(\Omega)} : k \in \{1, 2, 3, 4, 5\} \right\}$ , and let

$$U_k(t, z) = y_k(t, z) - ct - \|y_k^0\|_{L^\infty(\Omega)}.$$

It is clear that the function  $U_k$  satisfies the system

$$\begin{cases} \frac{\partial U_k(t, z)}{\partial t} = d_k \Delta U_k(t, z) + f_k(t, y(t, z)) - c, & t \in [0, t_f], \\ U_k(0, z, z') = y_k^0 - \|y_k^0\|_{L^\infty(\Omega)}. \end{cases}$$

This system admits a unique strong solution defined by

$$U_k(t, z) = \Gamma(t) \left( y_k^0 - \|y_k^0\|_{L^\infty(\Omega)} \right) + \int_0^t \Gamma(t-x) (f_k(y(x)) - c) dx,$$

where  $\Gamma(t)$  is an infinitesimal semigroup related to the operator  $d_k \Delta$ .

It comes that  $U_k(t, z) \leq 0$ , so  $y_k \leq ct + \|y_k^0\|_{L^\infty(\Omega)}$ .

Using the similar manner, we can prove that function  $V_k(t, z) = y_k(t, z) + ct + \|y_k^0\|_{L^\infty(\Omega)}$  is nonnegative. So,  $y_k \geq -ct - \|y_k^0\|_{L^\infty(\Omega)}$ , then  $|y_k(t, z)| \leq ct + \|y_k^0\|_{L^\infty(\Omega)}$ , which implies that

$$y_k \in L^\infty(Q) \quad \forall (t, z) \in [0, t_f] \times \Omega, \quad \text{for } k \in \{1, 2, 3, 4, 5\}. \quad (10)$$

Now, we establish that  $y_k \in L^\infty(0, t_f; H^1(\Omega))$  for all  $k \in \{1, 2, 3, 4, 5\}$ . Consider  $k \in \{1, 2, 3, 4, 5\}$ , and start from the equation

$$\frac{\partial y_k(t, z)}{\partial t} - d_k \Delta y_k(t, z) = f_k(t, y(t, z)), \quad (t, z) \in [0, t_f] \times \Omega.$$

We have

$$\int_0^t \int_\Omega \left( \frac{\partial y_k(t, z)}{\partial t} - d_k \Delta y_k(t, z) \right)^2 dz ds = \int_0^t \int_\Omega (f_k(t, y(t, z)))^2 dz ds.$$

By employing Green's formula, we arrive at

$$\begin{aligned} & \int_0^t \int_\Omega \left( \frac{\partial y_k}{\partial t} \right)^2 dz ds + d_k^2 \int_0^t \int_\Omega (\Delta y_k)^2 dz ds \\ &= 2d_k \int_0^t \int_\Omega \frac{\partial y_k}{\partial t} \times \Delta y_k dz ds + \int_0^t \int_\Omega (f_k(t, y_k))^2 dz ds \\ &= d_k \int_\Omega |\nabla y_k^0|^2 dz - d_k \int_\Omega |\nabla y_k|^2 dz + \int_0^t \int_\Omega (f_k(t, y_k))^2 dz ds. \end{aligned}$$

Since  $y_k^0 \in H^2(\Omega)$  and  $\|y_k\|_{L^\infty(Q)}$  are bounded independently of  $u$ , it follows that

$$y_k \in L^\infty(0; t_f; H^1(\Omega)), \quad \text{for } k \in \{1, 2, 3, 4, 5\}. \quad (11)$$

Based on (9), (10), and (11), it is determined that the inequality presented in (8) holds.

Furthermore, we conclude that the solution  $(y_1, y_2, y_3, y_4, y_5)$  remains non-negative using arguments similar to those employed for the Field-Noyes equations in [19]. Consider the set

$$\Pi = \{(y_1, y_2, y_3, y_4, y_5) : 0 \leq y_k \leq D \text{ for } k \in \{1, 2, 3, 4, 5\}\},$$

and define the convex functions  $F_k$  over  $\Pi$  as  $F_k(y_1, y_2, y_3, y_4, y_5) = -y_k$ . This leads to the following relationships:

$$\begin{aligned} \nabla(F_1) \cdot f|_{y_1=0} &= \nabla(-y_1) \cdot f|_{y_1=0} = -\Lambda \leq 0, \\ \nabla(F_2) \cdot f|_{y_2=0} &= \nabla(-y_2) \cdot f|_{y_2=0} = -(1-u)\alpha_2 y_1 y_3 \leq 0, \\ \nabla(F_3) \cdot f|_{y_3=0} &= \nabla(-y_3) \cdot f|_{y_3=0} = -\beta y_2 \leq 0, \\ \nabla(F_4) \cdot f|_{y_4=0} &= \nabla(-y_4) \cdot f|_{y_4=0} = -\eta y_3 \leq 0, \\ \nabla(F_5) \cdot f|_{y_5=0} &= \nabla(-y_5) \cdot f|_{y_5=0} = -\theta y_4 \leq 0. \end{aligned}$$

As shown in [19], the set  $\Pi$  is positively invariant.  $\square$

## 5 Existence of an optimal control

In this part, we aim to establish the presence of an optimal control for minimizing cost function (5) subject to the reaction diffusion system outlined in (2)–(4) with  $u \in U_{ad}$ . The primary outcome we seek to demonstrate in this section is as follows.

**Theorem 2.** Given the assumptions outlined in Theorem 1, the optimal control problem (2)–(5) possesses an optimal solution denoted as  $(y^*, u^*)$ .

*Proof.* Since  $u$  and  $y_k$  are uniformly bounded in  $L^\infty(Q)$  for  $k \in \{1, 2, 3, 4, 5\}$ , the infimum of the cost function is ensured. Let  $C^* = \inf_{u \in U_{ad}} C(y, u)$ . Consider a minimizing sequence  $\{u_n\} \subset U_{ad}$  such that  $\lim_{n \rightarrow +\infty} C(y^n, u_n) = C^*$ , where  $(y_1^n, y_2^n, y_3^n, y_4^n, y_5^n)$  is the solution of the system (2)–(3) corresponding to the control  $u_n$ . This leads to the following system:

$$\begin{cases} \frac{dy_1^n}{dt} = d_S \Delta y_1^n + \Lambda - (1 - u_n) [\alpha_1 y_2^n + \alpha_2 y_3^n] y_1^n - dy_1^n, \\ \frac{dy_2^n}{dt} = d_E \Delta y_2^n + (1 - u_n) [\alpha_1 y_2^n + \alpha_2 y_3^n] y_1^n - (d + \beta) y_2^n, \\ \frac{dy_3^n}{dt} = d_I \Delta y_3^n + \beta y_2^n - (d + \delta_1 + \eta) y_3^n, \\ \frac{dy_4^n}{dt} = d_H \Delta y_4^n + \eta y_3^n - (d + \delta_2 + \theta) y_4^n, \\ \frac{dy_5^n}{dt} = d_R \Delta y_5^n + \theta y_4^n - dy_5^n, \end{cases} \quad (12)$$

where  $\frac{\partial y_1^n}{\partial v} = \frac{\partial y_2^n}{\partial v} = \frac{\partial y_3^n}{\partial v} = \frac{\partial y_4^n}{\partial v} = \frac{\partial y_5^n}{\partial v} = 0$  on  $Q$ .

Given that  $H^1(\Omega)$  is compactly embedded in  $L^2(\Omega)$ , we can conclude that  $y_k^n(t, z)$  is compact in  $L^2(\Omega)$  for  $k \in \{1, 2, 3, 4, 5\}$ .

Additionally, we need to establish that  $\{y_k^n(t, z), n \geq 1\}$  is equicontinuous in  $C([0, t_f], L^2(\Omega))$ .

The boundedness of  $\frac{\partial y_k^n}{\partial t}$  in  $L^2(Q)$  implies the existence of a positive constant  $h$  such that

$$\left| \int_{\Omega} (y_k^n)^2(t, z) dz - \int_{\Omega} (y_k^n)^2(x, z) dz \right| \leq h|t - x|.$$

Hence, by the Ascoli–Arzela Theorem (see [5]), we can confirm that  $y_k^n$  is compact in  $C([0, t_f], L^2(\Omega))$ . Consequently,  $y_k^n \rightarrow y_k^*$  uniformly in  $L^2(\Omega)$  with respect to  $t$ .

Considering the boundedness of  $\Delta y_k^n$  in  $L^2(Q)$ , there exists a subsequence, denoted again as  $\Delta y_k^n$ , that converges weakly in  $L^2(Q)$ . Therefore, for all distributions  $\varphi$ ,

$$\int_Q \varphi \Delta y_k^n = \int_Q y_k^n \Delta \varphi \rightarrow \int_Q y_k^* \Delta \varphi = \int_Q \varphi \Delta y_k^*.$$

This implies that  $\Delta y_k^n \rightarrow \Delta y_k^*$  weakly in  $L^2(Q)$ . Furthermore,  $\frac{\partial y_k^n}{\partial t} \rightarrow \frac{\partial y_k^*}{\partial t}$  weakly in  $L^2(Q)$ , and  $y_k^n \rightarrow y_k^*$  weakly in  $L^2(0, t_f; H^2(\Omega))$  and  $y_k^n \rightarrow y_k^*$  weakly in  $L^\infty(0, t_f; H^1(\Omega))$ .

Since  $y_1^n y_2^n - y_1^* y_2^* = (y_1^n - y_1^*) y_2^n + y_1^* (y_2^n - y_2^*)$ , we deduce that  $y_1^n y_2^n \rightarrow y_1^* y_2^*$  in  $L^2(Q)$ . As a result,  $u_n \rightarrow u^*$  in  $L^2(Q)$ . Furthermore, since  $U_{ad}$  is a closed set, it follows that  $u^* \in U_{ad}$ .

By taking the limit as  $n \rightarrow \infty$  in (12), we can establish that  $y^*$  is a solution to (7) associated with  $u^*$ . Thus,

$$\begin{aligned}
C(y^*, u^*) &= \int_0^{t_f} ay_3^*(t, z) dt dz + \frac{b}{2} \|u^*(t, z)\|_{L^2(Q)}^2 \\
&\leq \liminf \int_0^{t_f} ay_3^n(t, z) dt dz + \frac{b}{2} \|u^n(t, z)\|_{L^2(Q)}^2 \\
&\leq \lim \int_0^{t_f} ay_3^n(t, z) dt dz + \frac{b}{2} \|u^n(t, z)\|_{L^2(Q)}^2 = C^*.
\end{aligned}$$

This confirms that  $C$  reaches its minimum at  $(y^*, u^*)$ .  $\square$

## 6 Necessary optimality conditions

In this section, we will delve into the optimality conditions for problem (2)–(5) with  $u \in U_{ad}$  and provide insights into the characterization of the optimal control. Consider an optimal pair denoted as  $(y^*, u^*)$ , and let  $u^\epsilon = u^* + \epsilon u$ , where  $\epsilon > 0$ , represents a control function satisfying  $u \in L^2(Q)$  and  $u \in U_{ad}$ . We denote the corresponding solutions of (2) associated with the controls  $u^\epsilon$  and  $u^*$  as  $y^\epsilon = (y_1^\epsilon, y_2^\epsilon, y_3^\epsilon, y_4^\epsilon, y_5^\epsilon)$  and  $y = (y_1^*, y_2^*, y_3^*, y_4^*, y_5^*)$ , respectively. We put

$$G = \begin{pmatrix} -d - (1 - u^*) (\alpha_1 y_2^* + \alpha_2 y_3^*) & -(1 - u^*) \alpha_1 y_1^* & -(1 - u^*) \alpha_2 y_1^* & 0 & 0 \\ (1 - u^*) (\alpha_1 y_2^* + \alpha_2 y_3^*) & (1 - u^*) \alpha_1 y_1^* - (d + \beta) & (1 - u^*) \alpha_2 y_1^* & 0 & 0 \\ 0 & \beta & -(d + \delta_1 + \eta) & 0 & 0 \\ 0 & 0 & \eta & -(d + \delta_2 + \eta) & 0 \\ 0 & 0 & 0 & \theta & -d \end{pmatrix}$$

and

$$P = \begin{pmatrix} (\alpha_1 y_2^* + \alpha_2 y_3^*) y_1^* \\ -(\alpha_1 y_2^* + \alpha_2 y_3^*) y_1^* \\ 0 \\ 0 \\ 0 \end{pmatrix}.$$

We have the following theorem.

**Theorem 3.** The mapping  $y : U_{ad} \rightarrow W^{1,2}([0, t_f], M(\Omega))$  for  $k \in \{1, 2, 3, 4, 5\}$  is Gateaux differentiable with respect to  $u^*$ . For any  $u \in U_{ad}$ ,  $y'_k(u^*) u = Y_k$ , consequently,  $Y = (Y_1, Y_2, Y_3, Y_4, Y_5)$  represents the unique solution to the problem given by

$$\frac{\partial Y}{\partial t} = AY + GY + uP \quad \text{subject to } Y(0, z) = 0.$$

*Proof.* We define  $Y_k^\epsilon = \frac{y_k^\epsilon - y_k^*}{\epsilon}$  for  $k \in \{1, 2, 3, 4, 5\}$ . By subtracting the systems corresponding to  $y_k^\epsilon$  and  $y_k^*$ , we derive the following equation:

$$\frac{\partial Y^\varepsilon}{\partial t} = AY^\varepsilon + G^\varepsilon Y^\varepsilon + uP \text{ subject to } Y^\varepsilon(0, z) = 0, \quad \text{for all } z \in \Omega$$

with

$$G^\varepsilon = \begin{pmatrix} -d - (1 - u^\varepsilon)(\alpha_1 y_2^* + \alpha_2 y_3^*) & -(1 - u^\varepsilon) \alpha_1 y_1^\varepsilon & -(1 - u^\varepsilon) \alpha_2 y_1^\varepsilon & 0 & 0 \\ (1 - u^\varepsilon)(\alpha_1 y_2^* + \alpha_2 y_3^*) & (1 - u^\varepsilon) \alpha_1 y_1^\varepsilon - (d + \beta) & (1 - u^\varepsilon) \alpha_2 y_1^\varepsilon & 0 & 0 \\ 0 & \beta & -(d + \delta_1 + \eta) & 0 & 0 \\ 0 & 0 & \eta & -(d + \delta_2 + \eta) & 0 \\ 0 & 0 & 0 & \theta & -d \end{pmatrix}.$$

Let  $(\Gamma(t), t \geq 0)$  be the semi-group generated by  $A$ . The solution to this system can be expressed as

$$Y^\varepsilon(t, z) = \int_0^t \Gamma(t - x)G^\varepsilon Y^\varepsilon(x, z)dx + \int_0^t \Gamma(t - x)uPdx.$$

Since the coefficients of the matrix  $G^\varepsilon$  are uniformly bounded with respect to  $\varepsilon$ , we can apply Grönwall's inequality to establish that  $Y_k^\varepsilon$  is bounded in  $L^2(Q)$ . Consequently,  $y_k^\varepsilon \rightarrow y_k^*$  in  $L^2(Q)$ . Taking the limit as  $\varepsilon \rightarrow 0$ , we obtain

$$\frac{\partial Y}{\partial t} = AY + GY + uP \quad \text{subject to } Y(0, z) = 0, \quad \text{for all } z \in \Omega.$$

Applying a similar approach, we conclude that  $Y_k^\varepsilon \rightarrow Y_k^*$  as  $\varepsilon \rightarrow 0$ . □

Consider the adjoint variable  $q = (q_1, q_2, q_3, q_4, q_5)$ , and let  $G^*$  represent the adjoint of the Jacobian matrix  $G$ . The dual system associated with our problem can be defined as follows:

$$-\frac{\partial q}{\partial t} - Aq - G^*q = D^*D\psi \quad \text{subject to } q(t_f, z) = 0, \quad (13)$$

where

$$D = \begin{pmatrix} 0 & 0 & 0 & 0 & 0 \\ 0 & 0 & 0 & 0 & 0 \\ 0 & 0 & 1 & 0 & 0 \\ 0 & 0 & 0 & 0 & 0 \\ 0 & 0 & 0 & 0 & 0 \end{pmatrix} \quad \text{and} \quad \psi = \begin{pmatrix} 0 \\ 0 \\ a \\ 0 \\ 0 \end{pmatrix}.$$

**Lemma 1.** Under the conditions of Theorem 1, if  $(y^*, u^*)$  represents an optimal pair, then there exists a unique strong solution denoted as  $q \in W^{1,2}([0, t_f], M(\Omega))$  for the dual system (13). Specifically, the components  $q_k \in L^2(0, t_f; H^2(\Omega)) \cap L^\infty(0, t_f; H^1(\Omega))$ , where  $k = \{1, 2, 3, 4, 5\}$ .

*Proof.* This lemma can be established by introducing a change of variable  $t' = t_f - t$  and employing a similar manner as demonstrated in the proof of Theorem 3.  $\square$

By employing linkages between the state and adjoint equations, objective functional, and standard optimality approaches, we are able to characterize the control optimal and get the necessary conditions for the optimal control problem.

**Theorem 4.** If there exists an optimal control  $u^*$  and its corresponding solution  $y^* \in W^{1,2}([0, t_f]; M(\Omega))$ , then the optimal control  $u^*$  can be expressed as

$$u^* = \min \left( u_{\max}, \max \left( 0, \frac{(q_2 - q_1)(\alpha_1 y_2^* + \alpha_2 y_3^*) y_1^*}{b} \right) \right). \quad (14)$$

*Proof.* Let  $(y^*, u^*)$  be an optimal pair. Let  $u^\varepsilon = u^* + \varepsilon h \in U_{ad}$  with  $h \in L^2(\Omega)$  and  $y^\varepsilon$  be the corresponding state solution. We get

$$\begin{aligned} C'(u^*)(h) &= \lim_{\varepsilon \rightarrow 0} \frac{1}{\varepsilon} (C(u^\varepsilon) - C(u^*)) \\ &= \lim_{\varepsilon \rightarrow 0} \frac{1}{\varepsilon} \left( a \int_0^{t_f} \int_\Omega (y_3^\varepsilon - y_3^*) dz dt + \frac{b}{2} \int_0^1 \int_\Omega ((u^\varepsilon)^2 - (u^*)^2) dz dt \right) \\ &= \lim_{\varepsilon \rightarrow 0} \left( a \int_0^{t_f} \int_\Omega \left( \frac{y_3^\varepsilon - y_3^*}{\varepsilon} \right) dz dt + \frac{b}{2} \int_0^1 \int_\Omega (2hu^* + \varepsilon h^2) dz dt \right). \end{aligned}$$

Since  $\lim_{\varepsilon \rightarrow 0} \frac{y_3^\varepsilon - y_3^*}{\varepsilon} = \lim_{\varepsilon \rightarrow 0} \frac{y_3(u^* + \varepsilon h) - y_3^*}{\varepsilon} = Y_3$ ,  $\lim_{\varepsilon \rightarrow 0} y_3^\varepsilon = y_3^*$  and  $y_3^\varepsilon, y_3^* \in L^\infty(Q)$ , it follows that  $C$  is Gateaux differentiable with respect to  $u^*$ , and we obtain

$$\begin{aligned} C'(u^*)(h) &= \int_0^{t_f} \int_\Omega a Y_3 dz dt + b \int_0^{t_f} \int_\Omega h u^* dz dt \\ &= \int_0^{t_f} \langle D\psi, DY \rangle dt + \int_0^1 \langle bu^*, h \rangle_{L^2(\Omega)} dt. \end{aligned}$$

If we put  $h = v - u^*$ , then

$$C'(u^*)(v - u^*) = \int_0^{t_f} \langle D\psi, DY \rangle dt + \int_0^1 \langle bu^*, v - u^* \rangle_{L^2(\Omega)} dt.$$

Since

$$\begin{aligned}
\int_0^{t_f} \langle D\psi, DY \rangle dt &= \int_0^{t_f} \langle D^* D\psi, Y \rangle dt \\
&= \int_0^{t_f} \left\langle -\frac{\partial q}{\partial t} - Aq - G^* q, Y \right\rangle dt \\
&= \int_0^{t_f} \left\langle q, \frac{\partial Y}{\partial t} - AY - GY \right\rangle dt \\
&= \int_0^{t_f} \langle q, P(v - u^*) \rangle dt \\
&= \int_0^{t_f} \langle P^* q, v - u^* \rangle_{L^2(\Omega)} dt,
\end{aligned}$$

and  $U_{ad}$  is convex. Therefore,  $C'(u)(v - u) \geq 0$  for every  $v \in U_{ad}$ , which is equivalent to

$$\int_0^{t_f} \langle P^* q + bu^*, v - u^* \rangle_{L^2(\Omega)} dt \geq 0 \text{ for every } v \in U_{ad}.$$

So,  $bu^* = -P^* q$ , thus  $u^* = \frac{(q_2 - q_1)(\alpha_1 y_2^* + \alpha_2 y_3^*) y_1^*}{b}$ . Since  $u^* \in U_{ad}$ , we have that (14) holds.  $\square$

## 7 Numerical simulation and presentation of the results

To achieve the interest of optimal control and evaluate the precision of our spatio-temporal model with and without control, we carried out a numerical simulation of our optimal control problem in the context of modeling the spread of disease. We adopt a rigorous methodological approach. Our optimality system is formulated by state equations with initial and boundary conditions (2)–(4), adjoint equations with transversality conditions (13), and a characterization of optimal control (14). To solve this system, we use the forward-backward scanning method in an iterative process. The temporal discretization of the state equations is carried out using the explicit Euler method, while the adjoint equations are solved retroactively in time. The space considered, representing a city  $\Omega = 50Km^2$ , is initially ( $t = 1$  day) populated randomly in the city, and it is assumed that the epidemic began to spread randomly in different areas of the city. The results will be presented as follows.

The values of the parameters connected to our spatio-temporal model with and without control are presented in Table 3.



Table 3: Parameters for the model without and with control.

Parameters	Values
$(\Lambda, d, \alpha_1, \alpha_2, \beta, \delta_1, \delta_2, \eta, \theta)$	$(0.06, 0.125, 0.65, 0.65, 0.5, 0.0001, 0.001, 0.05, 0.02)$
$(d_S, d_E, d_I, d_H, d_R)$	$(0.2, 0.2, 0.2, 0.2, 0.2)$

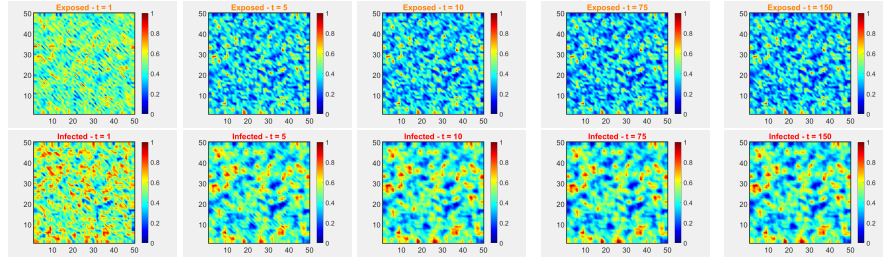


Figure 2: The behavior of compartments  $E$  and  $I$  without control

Before the enforcement of control measures, a pervasive presence of asymptomatic infections was observed in multiple locations throughout the region, suggesting a widespread dissemination of the epidemic within the city. Figure 4 illustrates a persistent high percentage of asymptomatic cases, consistently standing at 11% of the total population over time. This phenomenon played a role in the formation of a substantial cluster of symptomatic individuals across the city, comprising 31% of the total population. The visual representation underscored the extensive transmission of the infection in various areas of the city.

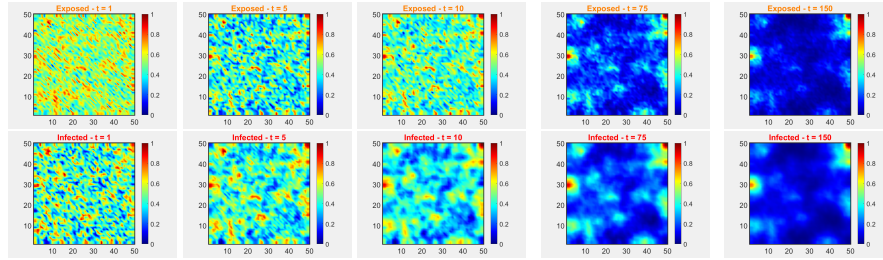


Figure 3: The behavior of compartments  $E$  and  $I$  with control

After the enforcement of stringent control measures, a noticeable transformation has taken place in the landscape of the epidemic. These measures, which strategically aimed to curtail the widespread prevalence of asymptomatic infections in various locations across the region, including crucial components such as reducing social interactions, conducting safety campaigns to discourage migration, and promoting health precautions to minimize virus transmission. The proactive interventions have resulted in a significant decrease in the overall percentage of asymptomatic cases, plummeting from the initial 11% to a mere 0.2%. Consequently, there has been a substantial reduction in the number of symptomatic individuals, with the affected population now comprising only 0.3% of the total. This positive development indicates the effectiveness of the implemented controls in containing the spread of the disease and alleviating its impact on the population. The newly established situation reflects a more controlled and manageable scenario, underscoring the success of the measures in restricting the transmission of the infection within the city.

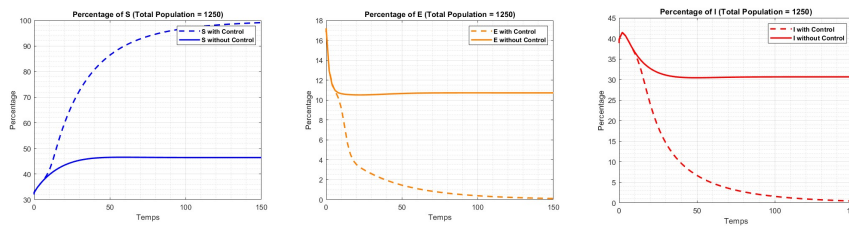


Figure 4: The percentage distribution of compartments  $S$ ,  $E$ , and  $I$  relative to the total population

## 8 Conclusion

The spatio-temporal model used in this work captures population size, movement models, and social relationships that are important in the evolution of EG.5 virus transmission, and as our study suggests, we now understand the role and potential of controls using intervention strategies, such as advocacy campaigns, creating social barriers, and focused testing on, to prevent the spread of the virus while reducing associated costs and societal disorders.

In conclusion, our analysis of this spatio-temporal epidemiological model contributes to well-known decision analyses and important mechanisms of epidemic development. This approach has the potential to combine rigorous mathematical analysis with real data to determine effective targeted therapies, ultimately supporting global efforts to combat the virus and protect humanity wall. Finally, to be more accurate and effective models, we can improve these models by combining other factors such as age, socio-economic characteristics and behavioral models. Additionally, efforts should be made to improve the data collection system and to develop reports that will provide modern, reliable data for accurate sampling, so that we can develop a reduction strategy epidemic and protect human health.

## Acknowledgements

Authors are grateful to there anonymous referees and editor for their constructive comments.

## Conflicts of interest

The authors declare no conflicts of interest.

## References

- [1] Abbasi, Z., Zamani, I., Mehra, A.H.A., Shafieirad, M. and Ibeas, A. *Optimal control design of impulsive SQEIR epidemic models with ap-*

- plication to COVID-19*. Chaos Solit. Fractals. 139 (2020) 110054.
- [2] El Alami Laaroussi, A. and Rachik, M. *On the regional control of a reaction-diffusion system SIR*. Bull. Math. Biol. 82 (2020) 1–25.
- [3] Aldila, D., Padma, H., Khotimah, K., Desjwiandra, B. and Tasman, H. *Analyzing the MERS disease control strategy through an optimal control problem*. Int. J. Appl. Math. Comput. Sci. 28(1) (2018) 169–184.
- [4] Athans, M. and Falb, P.L. *Optimal control: An introduction to the theory and its applications.*, Dover Publications, 2006.
- [5] Brezis, H., Ciarlet, P.G. and Lions, J.L. *Analyse fonctionnelle: théorie et applications*, vol 91. Dunod, Paris, 1999.
- [6] Chinchuluun, A., Pardalos, P.M., Enkhbat, R., and Tseveendori, I, Eds., *Optimization and optimal control: Theory and applications*, vol. 39, Springer, 2010.
- [7] Drosten, C., Seilmaier, M., Corman, V.M., Hartmann, W., Scheible, G., Sack, S., Guggemos, W., Kallies, R., Muth, D., Junglen, S. and Müller, M.A. *Clinical features and virological analysis of a case of Middle East respiratory syndrome coronavirus infection*. Lancet. Infect. Dis. 13 (2013) 745–751.
- [8] Guery, B., Poissy, J., El Mansouf, L., Séjourné, C., Ettahar, N., Lemaire, X., Vuotto, F., Goffard, A., Behillil, S., Enouf, V. and Caro, V. *Clinical features and viral diagnosis of two cases of infection with Middle East respiratory syndrome coronavirus: A report of nosocomial transmission*. Lancet 381(9885) (2013) 2265–2272.
- [9] Khajji, B., Kada, D., Balatif, O. and Rachik, M. *A multi-region discrete time mathematical modelling of the dynamics of Covid-19 virus propagation using optimal control*. J. Appl. Math. Comput. 64(1-2) (2020) 255–281.
- [10] Kim, Y., Lee, S., Chu, C., Choe, S., Hong, S. and Shin, Y. *The characteristics of Middle Eastern respiratory syndrome coronavirus transmission dynamics in South Korea*. Osong Public Health Res. Perspect. 7(1) (2016) 49–55.

- [11] Kouidere, A., Khajji, B., El Bhih, A., Balatif, O. and Rachik, M. *A mathematical modeling with optimal control strategy of transmission of covid-19 pandemic virus*. Commun. Math. Biol. Neurosci., 2020 (2020), Article ID 24.
- [12] Laaroussi, A.E.A., Ghazzali, R., Rachik, M. and Benrhila, S. *Modeling the spatiotemporal transmission of Ebola disease and optimal control: a regional approach*. Int. J. Dynam. Control, 7 (2019) 1110–1124.
- [13] Liberzon, D. *Calculus of Variations and Optimal Control Theory. A Concise Introduction*, Princeton University Press, Princeton, NJ, USA, 2012.
- [14] Madubueze, C.E., Dachollom, S. and Onwubuya, I.O. *Controlling the spread of covid-19: Optimal control analysis*. Comput. Math. Methods Med. (2020) Article ID 6862516.
- [15] El Mehdi, M., Said, M., Bouchaib, K., Omar, B. and Mostafa, R. *Mathematical Study Aiming at Adopting an Effective Strategy to Coexist with Coronavirus Pandemic*. J. Math. Comput. Sci. 11(1) (2021) 44–60.
- [16] Perkins, T.A. and España, G. *Optimal control of the COVID-19 pandemic with non-pharmaceutical interventions*. Bull. Math. Biol. 82(9) (2020) 118.
- [17] Pontryagin, L.S. *Mathematical theory of optimal processes*, John Wiley and Sons, London, UK, 1962.
- [18] Sari, R.A., Habibah, U. and Widodo, A., *Optimal control on model of SARS disease spread with vaccination and treatment*. J. Exp. Life Sci. 7(2) (2017) 61–68
- [19] Smoller, J. *Shock waves and reaction-diffusion equations*, Grundlehren der mathematischen Wissenschaften, 258, (GL, volume 258) Springer-Verlag, New York, 1994.
- [20] Stengel, R.F, *Optimal control and estimation*, Dover, New York, NY, USA, 1994.

- [21] Tahir, M., IS, A.S., Zaman, G. and Khan, T. *Prevention strategies for mathematical model MERS-Corona virus with stability analysis and optimal control*. J. Nanosci. Nanotechnol. Appl. 1(1) (2019) 1.
- [22] Vrabie, I.I.  *$C0$ -semigroups and applications*, North-Holland Mathematics Studies, 191, North-Holland Publishing Co., Amsterdam, Volume 191 (2003) 1–373.
- [23] Yang, C. and Wang, J. *A mathematical model for the novel coronavirus epidemic in Wuhan, China*. Math. Biosci. Eng. 17(3) (2020) 2708–2724.
- [24] Zine, H., Adraoui, A.E. and Torres, D.F. *Mathematical analysis, forecasting and optimal control of HIV/AIDS spatiotemporal transmission with a reaction diffusion SICA model*. AIMS Mathematics 7(9) (2022) 16519–16535.